Nat. Hazards Earth Syst. Sci. Discuss., 1, 4115–4154, 2013
www.nat-hazards-earth-syst-sci-discuss.net/1/4115/2013/
doi:10.5194/nhessd-1-4115-2013

Natural Hazards and Earth System Sciences Discussions
Open Access

The characteristics of lightning risk and zoning in Beijing simulated by a risk assessment model

H. Hu[1], J. Wang[2], and J. Pan[2]

[1]Institute of Urban Meteorology, CMA, Beijing, China
[2]Beijing Meteorological Bureau, Beijing, China

Received: 7 February 2013 – Accepted: 11 June 2013 – Published: 16 August 2013

Correspondence to: H. Hu (hbhu@ium.cn)

Published by Copernicus Publications on behalf of the European Geosciences Union.

Abstract

In this study, the Cloud-to-Ground (CG) lightning flash/stroke density has been derived from the Lightning Location Finder (LLF) data recorded in recent years. Meanwhile, the vulnerability on land surfaces has been assessed by the classification of the building, outdoor area under the building canopy and open-field area, which makes it convenient to deduce the location factor and confirm the protective capability. Then, the number of dangerous lightning event can be estimated by product of the CG stroke density and vulnerability. Although the human beings and all their material properties are identically exposed to lightning, the lightning casualty risk and property loss risk have been assessed respectively due to their vulnerability discrepancy. The analysis of the CG flash density in Beijing revealed that the JuMaHe river-valley in the southwestern region, the ChangPing–ShunYi zone downwind of the Beijing metropolis, and the mountainous PingGu–MiYun zone near the seashore are the most active lightning areas, with densities greater than 1.5 fl km^{-2} yr^{-1}. Moreover, the mountainous northeastern, northern, and northwestern rural areas are relatively vulnerable to lightning due to the ability of high elevation terrain to attract lightning and the lack of protection measures. In contrast, lightning incidents by indirect lightning are most likely to occur in urban areas with high population density and aggregated properties, and the property damages caused by lightning are more extensive than those in suburban and rural areas. However, casualty incidents caused by direct lightning strokes seldom occur in urban areas. On the other hand, the simulation based on the Lightning Risk Assessment Model (LRAM) demonstrates that the casualty risk is higher in rural, whereas the property loss risk is higher in urban, and this conclusion is also supported by the historical casualty and damage reports.

NHESSD
1, 4115–4154, 2013

1 Introduction

Lightning severely threatens the safety of human beings and their property (Elsom, 1993, 2001; Holle et al., 1996, 2005; Curran et al., 2000; Zhang et al., 2011) and has been recognized as one of the most dangerous natural disasters by the International Decade for Natural Disaster Reduction (IDNDR) (Ma et al., 2008). Lightning causes disasters in a straightforward manner in that anything struck by lightning stroke can result in casualties and damages (Curran et al., 2000). Obviously, the lightning risk is related to regional lightning activity, especially the CG flash density (Changnon, 1992; Baker, 1999; Williams, 2005). The Lightning Location Finder (LLF) data and the data collected by the satellite remote sensor of the Optical Transient Detector (OTD) and Lightning Imaging Sensor (LIS) are all available to deduce the lightning density and the associated climatic characteristics of lightning activity (Christian et al., 2003; Tao and Meng, 1996; Bovalo et al., 2012). Tao and Zhao (1993) summarized the temporal-spatial distribution of lightning in northern China with the Lightning Location Finder (LLF) data and concluded that lightning activity can be substantially influenced by mountain spreading and river-valley stretching. Christian et al. (2003) found that the annual flash count translates to an average of 44 ± 5 lightning flashes (intra-cloud and cloud-to-ground combined) occurring around the globe every second. Clearly, deducing the distribution of lightning density and disclosing the lightning activity, which is essential for a lightning risk assessment, are possible with the development of observatory techniques.

To help with lightning avoidance and mitigation, the lightning risk assessment is performed to determine where a lightning incident is most likely to occur (Meyer et al., 2009). Theoretically, lightning disasters are thought to be the result of interactions between their causative factors and exposure (Kaplan and Garrick, 1981; Smith, 1996; Garrick, 2002). The CG flash stroke is the direct cause of a lightning incident, as the lightning risk majorly related to the CG flash/stroke density (Fuquay et al., 1967; Lopez et al., 1997; Bogdan and Burcea, 2010). On the other hand, the population and its properties are also recognized as being the basic components of exposure to lightning

NHESSD
1, 4115–4154, 2013

as the lightning risk is considerably influenced by the distribution of population density (Holle et al., 2005; Wisdom, 2009; Zhang et al., 2011).

Vulnerability is another crucial factor of lightning risk (Ashley and Gilson, 2009). To assess the vulnerability, dividing the land surface into the classifications of building, the outdoor area under the building canopy and the open-field area is resonable because the protective capability and location factors which determine the susceptibility to lightning differ in these areas, and the methology of deducing these factors is in diversity. In a building, for example, factors such as its elevation, geometrical shape and height all influence lightning attraction and affect the building's vulnerability to lightning (Rizk, 1994; Petrov and D'Alessandro, 2002; Sonia and Gerard, 2005). Thus, introducing the technology of Geographical Information Systems (GIS) in lightning risk assessment is desirable to make it easier to locate these classified areas, estimate their ability to collect lightning, and assess the protective capability of individual building.

The Lightning Risk Assessment Model (LRAM) has been developed to calculate the average Annual Number of Dangerous Lightning Event (ANDLE), lightning casualty risk, and property loss risk supported by GIS, aiming to explore the characteristics of lightning risk and its zoning. Meanwhile, the model simulates the lightning risk with the parameterization of the CG flash/stroke density, vulnerability, and exposure to lightning. It should be noted that some critical factors associated with the lightning risk, such as human behavior, location and activity, are very difficult to quantify and may be negligible (Renn, 1998). However, the availability of the model would be capable of fitting the risk value by repeatedly modifying the input parameters in the simulation until it runs satisfactorily. After all, the simulation demonstrates the hypothesis of the lightning risk recognition in urban and rural areas in which the lightning casualty risk is higher in rural areas, whereas the property loss risk is higher in urban areas (Holle et al., 1996, 2005; Curran et al., 2000; Elsom, 1993, 2001; Wisdom, 2009).

2 Data description

2.1 The lightning location finder data

The climatological data recorded by 20 meteorological stations from 1961 to 2008 are used to count the annual number of thunder days from which the CG flash density can be converted using an empirical formula (Price and Rind, 1993) because the annual number of thunder days indicates the regional lightning activity (Gabriel and Changnon, 1989). Generally, the thunder days are recorded immediately by a weather observer when hearing the first peal of thunder, and this behavior obviously causes uncertainty (Changnon, 1992; Gabriel and Changnon, 1989). For this reason, the annual number of thunder days roughly reflects the lightning activity, and the converted CG flash density would not be suitable for risk assessment because of its low resolution and data uncertainty.

The lightning location finder data, recorded by the Beijing Meteorology Bureau, are substituted to calculate the CG lightning density. The data are composed of SAFIR (Système d'Alerte Foudre par Interférométrie Radioélectrique) data recorded in 2007 and ADTD (a lightning detection network of China Meteorological Administration) data from 2008 to 2011. In China, the SAFIR network consists of SAFIR3000 sensors, working by VHF interferometric technique for accurate angular localization of lightning discharge, both IC and CG lightning flashes, complemented with wide-band Low-Frequency (LF) for characterizing the lightning flashes to ground. The sensors have a detection efficiency estimated by the manufacturer at about 90 %. Orville Jr. et al. (1987) conclude that areas covered by two or more direction finders, detect 70 % of all lightning. Around Beijing, there are 3 SAFIR detection stations (Fig. 1), which the distances between two of the sensors are only about 126–145 km and allow an accuracy of lightning detection of better than 1 km.

The ADTD network consists of 232 sensors and the system employs the IMPACT method for lightning location, which combines the magnetic direction finding (MDF) and time-of-arrival (TOA) technique together (Bertram and Mayr, 2004). The overall

NHESSD
1, 4115–4154, 2013

detection efficiency of ADTD, the percentage of actual flashes observed by the network, is assumed to be in the 80–90 % range with the location accuracy better than 500 m. There are 5 detection stations of ADTD around Beijing (Fig. 1) where the detection efficiency could be higher than that of the other parts of China.

The detection of CG return strokes are grouped into CG flashes considering a multiplicity delay of 0.5 s in a radius of 7 km. All the +CG lightning flashes with peak current less than 15 kA have been classified as IC lightning (Biagi et al., 2007; Cummins et al., 2006, 2009). Because the return stroke and its subsequent CG strokes of a CG flash lead to lightning casualties and damages respectively, it is preferable to use the number of strokes or stroke density for calculating ANDLE.

The SAFIR contains (1) the altitude and longitude of the lightning position; (2) 5 types of lightning location discrimination, that is, 0: isolated point, 1: start point, 2: midpoint, 3: end of IC lightning, 4: return stroke, and 5: subsequent CG lightning stroke, which make it possible of selecting CG strokes records from the datasets. The ADTD contains the lightning latitude, longitude, intensity, slope, date time, and other features. The SAFIR recorded 35 171 CG flashes in 2007, and ADTD recorded 112 144 CG flashes in 4 yr, with an average annual CG flash density of approximately 1.7998 fl km^{-2} yr^{-1} in the 16 370 km^2 area of Beijing. The CG lightning data have been mapped in GIS, and the number of CG flash/stroke points contained in each grid-cell, substantially to be the CG flashes/strokes density, has been counted by a GIS statistical operator.

2.2 The Lightning Casualties and Damages Reports, and others

The Lightning Casualties and Damages Reports from 2001 to 2010, provided by the Beijing Lightning Devices Security Test Center, are introduced to explain the characteristics of lightning disasters. The reports keep the information of each lightning incident of its (1) date and time; (2) locality; (3) number and location of fatality/injury; (4) economic loss of the damage. A total of 440 lightning incidents, with 23 being casualty incidents, had been recorded. The locations of these incidents have also been mapped by the description of the reports (Fig. 11). The incident distribution map partially reflects the lightning risk characteristics and may help with testing and comparison of the assessment results.

Other data are also utilized including the following: (1) the GIS datasets in a high spatial resolution with map-scales of 1–2000 in urban settings and 1–50 000 in rural settings, besides the dataset of building with its attribute data containing information of the building type and number of floors, which are necessary for estimating the protective capability and the collection area of a building to lightning by building height; (2) the distribution map of population and GDP density derived from the Beijing statistical yearbook published in 2007; and (3) the Digital Elevation Map (DEM) with a resolution of 50 m ×50 m to determine the terrain features on the land surface.

The Lightning Risk Assessment Model (LRAM) is designed to perform on a GIS grid composed of 182 × 181 cells (Fig. 2), ranging from 115.3672° E to 117.5213° E and 39.4207° N to 41.0714° N, which covers the entire area of Beijing. The CG lightning flashes/strokes (fl/st), population (persons) and GDP (million Yuan) density are assigned to each 1 km × 1 km grid-cell. The model tries to utilize the input parameters together with the information abstracted from GIS data to quantitatively simulate the lightning risk, calculate the value of vulnerability, casualty risk and property loss risk for each grid-cell, and the gridded-data would be validated for final risk mapping and zoning (see Figs. 7–10).

3 The basic risk assessment formula

Theoretically, the disaster risk value R is considered to be the product of frequency N and exposure E (Smith, 1996), that is

$$R = N \cdot E \tag{1}$$

where the exposure E is usually substituted by population and properties, parameterized by population and Gross Domestic Product (GDP) density, and N is the frequency of dangerous lightning strikes, represented by the ANDLE N_x (times km^{-2} yr^{-1}), which is

$$N_x = K \cdot N_g \cdot A_d \tag{2}$$

where N_g is the CG stroke density, preferably obtained from the lightning location finder data (Tao et al., 1993; Zheng et al., 2005), A_d (m^2) is the equivalent collection area to lightning, and K is the correction factor, denoting the vulnerability involving protection measures and susceptibility to lightning.

4 The method of calculating ANDLE

Classifying the land surface into buildings, the outdoor areas under the building canopy and the open-field areas is necessary in calculating ANDLEs due to the convenience of measuring the collection areas of objects to lightning by certain geometrical shapes or heights, and estimating the location factor by elevation. Additionally, confirming the protective capability by the classification is favorable of distingushing the capability discrepancies in individual buildings. The classification also simplifies the model parameterization in calculating the number of dangerous lightning events, which can be accomplished on the GIS grid. Figure 2 shows samples of the classified areas and the GIS grid cells.

4.1 Estimating average ANDLEs of buildings

In built-up areas, the ANDLE of a building N_d (times yr^{-1}) can be estimated by

$$N_d = N_g \cdot A_d \cdot C_d \cdot P_d \times 10^{-6} \tag{3}$$

where A_d (m^2) is the collection area of a building to lightning, C_d is the location factor, and P_d is the protective factor. Except for the CG stroke density, N_g, obtained from the lightning location finder data, the other parameters can be deduced as follows.

NHESSD
1, 4115–4154, 2013

4.1.1 The collection area of a building to lightning

The capability of a building to collect lightning depends on the building location, height and the influence of the nearby buildings. Fundamentally, the dimension of the collection area is assumed to be three times of the building height (IEC62305, 2006). However, this area may intersect with that of the other buildings, and it should be measured by several cases.

The first case is a single building without any other nearby buildings; thus its collection area does not intersect with that of any other buildings (Fig. 3a). In this case, the collection area is determined by the geometrical buffer of the building in which the distance from the border of the buffer to the building edge is three times of the building height.

The second case is the collection areas of two buildings that intersect with each other (Fig. 3b). The allocation of the intersect area by the two buildings depends on the heights of the two buildings (Rizk, 1994), i.e. usually the higher building occupies a greater proportion of the intersect area, which is

$$A_d(\mathrm{A}) = S_{\mathrm{Buffer\,A}} - \left(1 - \frac{H_\mathrm{A}}{H_\mathrm{A} + H_\mathrm{B}}\right) \cdot S_{\mathrm{intersect}} = S_{\mathrm{Buffer\ A}} - \left(\frac{H_\mathrm{B}}{H_\mathrm{A} + H_\mathrm{B}}\right) \cdot S_{\mathrm{intersect}} \quad (4)$$

$$A_d(\mathrm{B}) = S_{\mathrm{Buffer\ B}} - \left(\frac{H_\mathrm{A}}{H_\mathrm{A} + H_\mathrm{B}}\right) \cdot S_{\mathrm{intersect}} \quad (5)$$

where $A_d(\mathrm{A})$ and $A_d(\mathrm{B})$ are the collection areas of buildings A and B, respectively (Fig. 3b), $S_{\mathrm{Buffer\,A}}$ and $S_{\mathrm{Buffer\ B}}$ are the respective buffer areas, H_A and H_B are the respective building heights, and $S_{\mathrm{intersect}}$ is the intersect area of buffers A and B. If the heights A and B are equal, the intersect area will be allocated equally, implying that their capability of collecting lightning is equivalent.

NHESSD
1, 4115–4154, 2013

The third case is the collection areas of more than two buildings that overlap with one another (Fig. 3c). Then, each collection area can be calculated by

$$A_d(1) = S_{buffer}(1) - \left(1 - \frac{H(1)}{\sum_{i=1}^{n} H(i)}\right) \cdot S_{overlap}(1) \tag{6}$$

...

$$A_d(n) = S_{buffer}(n) - \left(1 - \frac{H(n)}{\sum_{i=1}^{n} H(i)}\right) \cdot S_{overlap}(n) \tag{7}$$

where $A_d(1), \ldots,$ and $A_d(n)$ are the collection areas of buildings 1, ..., and n, respectively, $S_{Buffer\,(1)}, \ldots,$ and $S_{Buffer\,(n)}$ are the respective buffer areas, $S_{overlap}(1), \ldots,$ and $S_{overlap}(n)$ are the respective overlapping areas of each building buffer with the others, and $H(1), \ldots,$ and $H(n)$ are the respective building heights.

4.1.2 The location factor of building

The lightning attachment of a building is influenced to a certain degree by the topography of the building location, primarily by its elevation within a range of 250 m (IEC62305, 2006), where the relatively higher location can attract more ground lightning flashes/strokes than its surroundings. Herein, the Digital Elevation Map (DEM) is used to estimate the location factor value C_d, which is determined by the surrounding topography (see IEC62305, 2006, Part 2, p. 97).

4.1.3 The protective capability of building

The protective capability of building includes (1) the capability of protecting the live beings from injured by a lightning stroke, (2) protecting the building from physical damage, and (3) protecting the internal systems in the building. Substantially, these protective capabilities is represented by the casualty probability p_a, the physical damage probability p_b, and the internal systems failure probability p_c, respectively in risk estimation.

NHESSD
1, 4115–4154, 2013

However, the values of p_a, p_b, and p_c can be assigned according to the building and construction standard of lightning protection (IEC62305, 2006), which are critical for the risk simulations:

1. *The casualty probability*

   The casualty probability due to touch and step voltage by a lightning stroke to the building, depends on the building Lightning Protection Level (LPL), which can be determined by a function of typical protection measures (see IEC62305, 2006, Part 2, p. 105).

2. *The physical damage probability*

   The physical damage probability p_b in a building depend on the Lightning Protection Systems (LPS) level and the corresponding protection measures (see IEC62305, 2006, Part 2, p. 107).

3. *The internal systems failure probability*

   The Surge Protective Device (SPD) are designed to protect the internal systems of a building from damaged by direct/indirect lightning stroke. Accordingly, the internal system failure probability p_c primarily depends on the adopted coordinated SPD protection level (see IEC 62305, Part 2, p. 107).

4. *The quantification of the building protective capability*

   Quantifying the building protective capability by the building type is indispensable for the model parameterization. In order to determine the building protective capability, we have defined the protection measures that would be probably taken by 10 building types in Beijing (see Table 1). Most of these buildings are equipped with lightning rods, and some concrete steel buildings have iron infra-building and framework as the lead-in wire for lightning protection and thus possess a better capability of protecting the live beings from injured by ground lightning stroke.

NHESSD
1, 4115–4154, 2013

On the other hand, Installing Lightning Protection Systems (LPS) and Surge Protective Device (SPD) is often required to improve the lightning protection level. Nevertheless, in the 10 building types, only the special houses and general buildings would likely have possessed LPS protection measures, which would attain LPS I and LPS II to III level (Table 1), respectively. Fewer buildings have been designed SDP, and thus the capability of protecting material property is unsatisfactory, which explains why most of the lightning incidents would be prone to cause physical damages.

4.2 Estimating ANDLE of the outdoor area under the building canopy

Absolutely, the outdoor area under the building canopy is covered by the lightning collection area of the nearby buildings (Fig. 2 in shadow). However, the nearby buildings can unintentionally act as lightning rods for the area and intercept the lightning before impact, thereby leading to a very low probability of being struck by lightning stroke. The ANDLE N_{Dc} (times km^{-2} yr^{-1}) can be calculated by

$$N_{\text{Dc}} = N_{\text{g}} \cdot A_{\text{Dc}} \cdot C_{\text{Dc}} \times 10^{-6} \tag{8}$$

where the collection area A_{Dc} (m^2) equals total collection areas of the buildings subtracted from the areas occupied by the buildings in a grid-cell (Fig. 2), and the location factor C_{Dc} can be estimated by

$$C_{\text{Dc}} = \frac{h \cdot \sum_{i=1}^{n} S_{\text{buffer}}(i)}{\sum_{i=1}^{n} (S_{\text{buffer}}(i) \cdot H(i))} \tag{9}$$

where h is the constant height of one floor, $H(1), \ldots,$ and $H(n)$ are the nearby building heights, and $S_{\text{Buffer}}(1), \ldots,$ and $S_{\text{Buffer}}(n)$ are the respective buffer areas, denoting the collection areas of the nearby buildings. Undoubtedly, many of the nearby tall buildings will result in few lightning strokes because most lightning will be previously intercepted.

NHESSD
1, 4115–4154, 2013

4.3 Estimating ANDLE of an open field area not under a building canopy

Everything in an open field is thoroughly exposed to lightning, and thus the lightning risk is much higher than that under the building canopy. The ANDLE N_{Ds} (times km^{-2} yr^{-1}) is

$$N_{Ds} = N_g \cdot A_{Ds} \cdot C_{Ds} \times 10^{-6} \tag{10}$$

where the collection area A_{Ds} (m^2) equals the grid-cell area subtracted from the building collection areas in the grid (Fig. 2 in blank), and the location factor C_{Ds} can be estimated with the DEM (see Table 2). Apparently the location factor in this situation could be greater than that calculated by Eq. (9).

5 The implementation of lightning risk assessment model

In principle, the ANDLE is the index of causative factors, and the human beings and material properties are the exposure factors. However, the vulnerabilities of human beings and properties to lightning are not identical due to the obvious discrepancy in protective capability, resistance and loss rate (Holle et al., 1996, 2005; Curran et al., 2000). For risk identification and management, the lightning risk should be separated into casualty risk and property loss risk and assessed by the following procedures.

5.1 Lightning casualty risk

The ANDLE on land surface N is the accumulation of the ANDLEs of the buildings, outdoor areas under the building canopy and open field areas, which is

$$N = N_d + N_{Dc} + N_{Ds} = N_g \cdot (A_d \cdot C_d \cdot P_d + A_{Dc} \cdot C_{Dc} + A_{Ds} \cdot C_{Ds}) \times 10^{-6} \tag{11}$$

Herein, the protective capability of building p_d refers to casualty probability p_a, which is $P_d = P_a$.

NHESSD
1, 4115–4154, 2013

On the whole, the ANDLE is the product of the CG stroke density N_g and vulnerability V, and thus the vulnerability is

$$V = (A_d \cdot C_d \cdot P_d + A_{Dc} \cdot C_{Dc} + A_{Ds} \cdot C_{Ds}) \times 10^{-6} \quad (12)$$

Therefore, the casualty risk in grid cell R_p (persons times^{-1} km^{-2} yr^{-1}) is

$$R_p = N \cdot E_p = N_d \cdot l_t \cdot E_{p,\,d} + N_{Dc} \cdot l_{t,\,canopy} \cdot E_{p,\,canopy} + N_{Ds} \cdot l_{t,\,space} \cdot E_{p,\,space} \quad (13)$$

where $E_{p,\,d}$, $E_{p,\,canopy}$, $E_{p,\,space}$ are the exposure of population in the building, outdoor area under the building canopy and open-field area, respectively; E_p is the total population in the grid cell; N_d, N_{Dc}, and N_{Ds} are the respective ANDLE values for these areas, and l_t, $l_{t,\,canopy}$, and $l_{t,\,space}$ are the respective loss ratios. Let $l_{t,\,space} = l_{t,\,canopy} = 10^{-4}$, and $l_t = 10^{-6}$ (referenced to IEC 62305, 2006).

The population density in the classified areas would be estimated by two groups: the indoor and outdoor. The estimation depends on the ratio of the outdoor population variable at 0–24 h intervals within a day (Table 3). We estimate the indoor or outdoor population mainly by the ratio at the interval of 10–24 h because lightning is generally active at the interval of 12–22 h in Beijing (Zhou et al., 2009). Additionally, lightning incidents mostly occur in an interval of 10–24 h according to the historical damage reports (Fig. 4).

5.2 Lightning related property loss risk

In the formula of property loss risk assessment, the GDP density substitutes for the exposure, that is

$$R_g = N_g \cdot A_d \cdot C_d \cdot P_d \cdot E_g \cdot l_r \times 10^{-6} \quad (14)$$

where R_g (Yuan times^{-1} km^{-2} yr^{-1}) is the property loss risk, l_r is the property loss ratio, and E_g (Yuan km^{-2}) is the GDP density. The protective capability P_d refers to the

Discussion Paper | Discussion Paper | Discussion Paper | Discussion Paper |

NHESSD

1, 4115–4154, 2013

The characteristics of lightning risk and zoning in Beijing

H. Hu et al.

physical damage probability p_b and the internal system failure probability p_c, which is $P_d = p_b + p_c$, provided that the property is generally under the protection of a building.

The property loss ratio l_r refers to the ratio of expected damage loss C_l to the asset values threatened by lightning C, that is

$$l_r = \frac{C_l}{C}. \tag{15}$$

Given $C_l = R_g$, indicating the property loss risk substitute for the expected damage loss, the Eq. (14) can be

$$R_g = N_g \cdot A_d \cdot C_d \cdot P_d \cdot E_g \cdot \frac{R_g}{C} \times 10^{-6},$$
$$C = N_g \cdot A_d \cdot C_d \cdot P_d \cdot E_g \times 10^{-6}. \tag{16}$$

Then, we can estimate the asset values threatened by lightning C using Eq. (16), without knowing the loss ratio l_r. Thus, C denotes the amount of GDP under the threat of lightning based on Eq. (16). However, the damage loss C_l can be obtained from the damage reports, and the property loss ratio l_r would be estimated by Eq. (15).

5.3 The framework of the Lightning Risk Assessment Model (LRAM)

The simulation works out the average ANDLE N, vulnerability V, lightning casualty risk R_p and property loss risk R_g, by the procedure of data deriving, locating, and assessing (Fig. 5). The model depends on the data resources of (1) the statistical yearbook from which the exposure of population and GDP density is derived, (2) the lightning location finder data for calculating the CG stroke density, (3) the GIS mapping data for locating and classifying the land surface, and (4) the DEM for deducing the location factor. Particularly, the ANDLE is calculated out with the CG stroke density and vulnerability composed of the protective capability and location factor. Subsequently, the ANDLE overlapping with the population and GDP density can be used to obtain the lightning casualty risk and property loss risk, respectively.

NHESSD
1, 4115–4154, 2013

6 The risk simulation and analysis

6.1 The CG flash/stroke density

Based on the climatological data over a period of five decades, the annual lightning density in Beijing is 9.59 fl km^{-2} yr^{-1} (intra-cloud and cloud-to-ground combined), converted using an empirical formula (Price and Rind, 1993), which is approximately equal to that of the global annual lightning density (Christian et al., 2003); the CG flash density ranges from 1.6 to 2.4 fl km^{-2} yr^{-1}, 0.2606 of the lightning density (intra-cloud and cloud-to-ground combined), corresponding to the climatic characteristic of the lightning activity in a warm temperate zone at a ratio of 2/3 (Zhou et al., 2009).

Meanwhile, the CG flash density derived from lightning location finder data mostly ranges from 0.5 to 2 fl km^{-2} yr^{-1}. Three high density areas in which the CG flash density is greater than 1.5 fl km^{-2} yr^{-1} are identified (Fig. 6): the JuMaHe river-valley in the southwestern region (A), the ChangPing–ShunYi zone (B), and the PingGu–MiYun zone (C). The reason of the high CG flash density in JuMaHe river-valley is that the mountain ranges and rivers spreading around the river valley so that moisture is abundant at the bottom of the river valley, resulting in convergence of current flow and convective force, conditionally enhancing the convection (Tao and Zhao, 1993; Zheng et al., 2005; Bogdan and Burcea, 2010). However, the ChangPing–ShunYi zone is to the north of the Beijing metropolis, downwind of the summer monsoon, which results in a stronger convection (Mote et al., 2007; Stallins and Rose, 2008; Rose et al., 2008). The PingGu–MiYun zone near the BoHai seashore, is abundant in humidity and its spreading mountains also enhance the convection (Zheng et al., 2005). It is clear that lightning is relatively active in the mountainous rural areas of Beijing.

6.2 Lightning risk simulated by the model

6.2.1 Vulnerability

The model estimates the vulnerability using Eq. (13), and the result shows that in the mountainous northern and western regions, the vulnerability is still higher than that of the plains, where the urban area sprawls out from the center (Fig. 7). Indeed, in rural and suburban areas, the hill-shaped terrain can easily attract CG lightning due to point charge (Vogt, 2011). Additionally, in the speculation of protection against lightning, finding buildings for immediate sheltering in thunderstorms is relatively difficult in rural areas; furthermore, few rural dwellings have been equipped with lightning rods. In China, 97 % of the lightning fatalities and injuries occur in rural areas (Ma et al., 2008); meanwhile, our historical casualty reports reveal that the rural areas account for 91.3 % of the lightning fatalities and injuries reported from 2001 to 2010.

6.2.2 The average annual number of dangerous lightning event

Calculated using Eq. (12), the ANDLE is approximately more than 3.0 times $km^{-2}\,yr^{-1}$, even as high as 9.0 times $km^{-2}\,yr^{-1}$ in the mountainous rural areas but less than 0.3 times $km^{-2}\,yr^{-1}$ in urban areas; the number is absolutely higher in the mountainous areas due to its high CG flash/stroke density and vulnerability (Fig. 8). The ANDLE can be recognized as the causative factor not overlapping with exposure, and evidently it indicates a potential hazard, that anything staying in the high value area is more likely to be struck by lighting flashes/strokes than anywhere else. For the risk management, the significance of the zoning for ANDLE is that it clarifies where is prone to be struck by lightning so that necessary mitigation or protection measures should be adopted to reduce the risk.

NHESSD
1, 4115–4154, 2013

6.2.3 The lightning casualty risk

By Eq. (12), the casualty risk value R_p (persons km^{-2} yr^{-1}) is the product of ANDLE and the population density. The risk simulation demonstrates that even with the high population density, the R_p in urban areas is generally lower than that in the suburban or rural areas. Moreover, the distribution of the high R_p area significantly corresponds to that of the historical casualty incidents (Fig. 9). In detail, the R_p is generally less than 0.0845 persons km^{-2} yr^{-1} in most urban areas, an estimated return period of nearly 118 yr. In most rural areas, the R_p is more than 0.16867 persons km^{-2} yr^{-1}, with the maximum of 0.5876 persons km^{-2} yr^{-1}. Consequently, the buildings in urban are often concrete steel buildings equipped with lightning rods, which would be effective in protecting human beings, and finding a building as a lightning shelter is also easier in these areas, whereas there are sparsely spreading buildings in rural areas, mostly lack of lightning protection measures (Zhang et al., 2011). Additionally, in urban many high-rise buildings produce a lightning rod effect, reducing the probability of being struck by direct lightning. Hence, in risk simulation, we set the proportion of outdoor population on thunderstorm days relatively lower in urban areas and assume that majority of the outdoor population should be under the canopy of its nearby buildings, thus the calculated risk value is lower.

According to our historical casualty reports, most of the lightning fatalities or injuries occurred in the suburban or rural areas when working in the open field, sheltering under trees, riding bicycles, touring in outskirts, and other activities, what is in accordance with the findings of Holle et al. (1996, 2005), Curran et al. (2000), Wisdom (2009), and Zhang et al. (2011). In addition, it can be perceived that the sum of the casualty risk values R_p estimated by risk simulation is 29.649 persons yr^{-1} in Beijing, whereas there were 13 lightning fatalities and 38 injuries from 2001 to 2010 (5.44 casualties annual) by the historical casualties reports, indicating that the reports probably have underreported the actual lightning casualties (Lopez et al., 1997; Curran et al., 2000; Zhang, 2011). Of course, the model uncertainty should be another reason. However, the two values are still in the same magtitude order which means the casualty risk simulated by the model is somehow acceptable.

6.2.4 The property loss risk

In the simulation of property loss risk, the GDP density substitutes for the exposure to estimate the amount of GDP under the threat of lightning, using Eq. (16). The estimated values are generally greater than 0.83 million Yuan km^{-2} yr^{-1} in urban areas and lower than 0.135 million Yuan km^{-2} yr^{-1} in rural or suburban areas, obviously higher in urban areas (Fig. 1a). The sum of the values is 849.0671 million Yuan, while the annual lightning-related loss is 1.586 million Yuan in Beijing according to the damage reports, so the property loss ratio is 0.001868. Then, the property loss risk can be calculated out by Eq. (14), and this risk values are generally greater than 2000 (Yuan km^{-2} yr^{-1}) in urban areas and lower than 100 (Yuan km^{-2} yr^{-1}) in rural or subsurban areas (Fig. 1b), differing from that of the casualty risk. This finding can be explained by the high GDP density in urban, where the properties are more vulnerable to lightning, especially of electronic or electrical equipment, which can be destroyed by an induced current or electromagnetic pulse in lightning. Although the Lightning Protection Systems (LPS) and Surge Protective Device (SPD) can effectively protect these properties from damage by direct or secondary lightning strikes, these measures rarely become popular even in well-developed urban areas due to their expensiveness. Actually, only the building type of special houses is assigned to a SPD level (see Table 3) in the model simulation.

According to the damage reports, most of the property damage incidents occurred in urban areas (Fig. 11), in agreement with the model simulation, and these incidents were mostly related to electronic, electrical, and transmission equipment damages, with a proportion of 86 %. Meanwhile, the Average Annual Economic Loss Densities (AAELD, Yuan km^{-2} yr^{-1}) of the districts in Beijing have been obtained from the damage reports (Fig. 12). It indicates that the districts of central metropolis or highly urbanization areas usually have a high AAELD, such as DongCheng

NHESSD
1, 4115–4154, 2013

(11 054 Yuan km^{-2} yr^{-1}) and XuanWu (18 041 Yuan km^{-2} yr^{-1}); the districts of HaiDian (1869 Yuan km^{-2} yr^{-1}) and FengTai (4459 Yuan km^{-2} yr^{-1}), partially composed of suburban areas, their AAELDs are relative lower than that of the highly urbanized districts, and that of the suburban and rural districts are the lowest ones, such as YangQing (35 Yuan km^{-2} yr^{-1}) and MiYun (45 Yuan km^{-2} yr^{-1}). This characteristic is well in accordance with the property loss risk simulated by the model. Exceptional of ShiJingShan, a recognized urban district, its AAELD is 770 Yuan km^{-2} yr^{-1}, lower than that of some suburban or even rural districts, such as DaXing (932 Yuan km^{-2} yr^{-1}) and PingGu (2685 Yuan km^{-2} yr^{-1}). Probably, the reason is that ShiJingShan is majorly occupied by the military facilities which do not belong to the municipality, and the damage reports wouldn't cover these facilities. Thereby, the fronted problem is that the reports usually underestimate the lightning loss (Holle et al., 1996, 2005; Zhang et al., 2011) and they cann't accurately manifest the actual damage loss, which is critical for estimating property loss ratio, so a comprehensive approach of lightning loss investigating and data collecting is necessary for uncertainty reduction.

7 Summary and conclusion

The CG flash/stroke density derived from lightning location finder data rationally reflects the regional lightning activity of Beijing, and three relatively high CG flash density areas have been spotted, all in rural. Comparatively, the CG flash density converted from the annual number of thunder days is unsuitable for lightning risk assessment because of its low resolution and data uncertainty.

ANDLE companied with the vulnerability of suscepitibility and protective capability have been carried out by classifying the land surface into the building, outdoor area under the building canopy and open-field area. The classification makes it convenient of locating these areas and confirming the protective capability of individual building, which can be accomplished on a GIS platform. Consequently it has been found that in the mountainous northern or western areas, the vulnerability is higher than that in the urban areas, because the mountainous terrain in rural areas can easily attract lightning and the rural dwellings are mostly lack of protection measures. Also, the estimated ANDLE is higher in rural areas. The significance of ANDLE zoning is that it clarifies where is most likely to be threatened by lightning which is imperative for risk management.

The lightning risk has been separated into the casualty risk and property loss risk, due to the discrepancy in protective capability, resistance and loss rate. The casualty risk is assessed by the product of ANDLE and population density. Despite the high population density in urban areas, this risk value is generally lower in urban than that in rural, corresponding with the distribution of the historical casualty incidents. This finding can be explained by the better protective capability of the buildings and easily sheltering on thunderstorm days in urban, as well as lightning rod effect produced by high-rise buildings.

In the simulation of property loss risk, the amount of GDP under the threat of lightning is calculated out firstly. The property loss ratio is defined as the ratio of lightning-related loss to the amount of GPD under the threat of lightning, but its estimation would bring about uncertainty, because the damage reports usually underestimate the lightning loss, so a comprehensive collection of loss data is needed for uncertainty reduction. Nevertheless, with this property loss ratio, the risk assesement of property loss indicates that this risk values are generally greater in urban than that in rural or suburban areas, due to property aggregation in urban and vulnerability of material properties to lightning. According to the damage reports, most of the property damage incidents occurred in urban areas, and the values of average annual economic loss densities are still high among urban districts, corresponding to the distribution of the property loss risk simulated by the model.

Acknowledgements. This study has been supported by the National Natural Science Foundation of China (Project: 41175099), and the Beijing Natural Science Foundation of China (Project: 9102009).

References

Ashley, W. S. and Gilson, C. W.: A reassessment of US lightning mortality, B. Am. Meteorol. Soc., 90, 1501–1518, 2009.
Baker, M. B.: Relationships between lightning activity and various thundercloud parameters: satellite and modeling studies, Atmos. Res., 51, 221–236, 1999.
Bertram, I. and Mayr, G. J.: Lightning in the eastern Alps 1993–1999, part I: Thunderstorm tracks, Nat. Hazards Earth Syst. Sci., 4, 501–511, doi:10.5194/nhess-4-501-2004, 2004.
Biagi, C. J., Cummins, K. L., Kehoe, K. E., and Krider, E. P.: National lightning detection network (NLDN) performance in southern Arizona, Texas, and Oklahoma in 2003–2004, J. Geophys. Res., 112, D05208, doi:10.1029/2006JD007341, 2007.
Bogdan, A. and Burcea, C.: A cloud-to-ground lightning climatology for Romania, Mon. Weather Rev., 138, 579–591, doi:10.1175/2009MWR2975.1, 2010.
Bovalo, C., Barthe, C., and Bègue, N.: A lightning climatology of the South-West Indian Ocean, Nat. Hazards Earth Syst. Sci., 12, 2659–2670, doi:10.5194/nhess-12-2659-2012, 2012.
Changnon, S. A.: Relationships between thunderstorms and cloud-to-ground lightning in the United States, J. Appl. Meteorol., 32, 88–105, 1992.
Christian, H. J., Blakeslee, R. J., Boccippio, D. J., Boeck, W. L., Buechler, D. E., Driscoll, K. T., Goodman, S. J., Hall, J. M., Koshak, W. J., Mach, D. M., and Stewart, M. F.: Global frequency and distribution of lightning as observed from space by the Optical Transient Detector, J. Geophys. Res., 108, 4005, doi:10.1029/2002JD002347, 2003.
Cummins, K. L. and Murphy, J. M.: An overview of lightning locating systems: history, techniques, and data uses, with an in depth look at the US NLDN, IEEE T. Electromagn. C., 51, 499–518, 2009.
Cummins, K. L., Cramer, J. A., Biagi, C. J., Krider, E. P., Jerauld, J., Uman, M. A., and Rakov, V. A.: The U.S. National Lightning Detection Network: Post-upgrade status, presented at 2nd Conf. on Meteorological Appl. of Lightning Data, AMS Annual Meeting, Atlanta, available at: https://ams.confex.com/ams/pdfpapers/105142.pdf, last access: 31 January 2013, 2006.
Curran, E. B., Holle, R. L., and Lopez, R. E.: Lightning casualties and damages in the United States from 1959 to 1994, J. Climate, 13, 3448–3464, 2000.
Elsom, D. M.: Deaths caused by lightning in England and Wales, 1852–1990, Weather, 48, 83–90, 1993.

NHESSD
1, 4115–4154, 2013

The characteristics of lightning risk and zoning in Beijing

H. Hu et al.

Elsom, D. M.: Deaths and injuries caused by lightning in the United Kingdom: Analyses of two databases, Atmos. Res., 56, 325–334, 2001.
Fuquay, D. M., Baughman, R. G., Taylor, A. R., and Hawe, R. G.: Characteristics of seven lightning discharges that caused forest fires, J. Geophys. Res., 72, 6371–6373, doi:10.1029/JZ072i024p06371, 1967.
Gabriel, K. R. and Changnon, S. A.: Temporal features in thunder days in the United States, Climatic Change, 15, 455–477, 1989.
Garrick, B. J.: The use of risk assessment to evaluate waste disposal facilities in the United States of America, Safety Sci., 40, 135–151, 2002.
Holle, R. L., Lopez, R. E., Arnold, L. J., and Endres, J.: Insured lightning-caused property damage in three western states, J. Appl. Meteorol., 35, 1344–1351, 1996.
Holle, R. L., López, R. E., and Navarro, B. C.: Deaths, injuries, and damages from lightning in the United States in the 1890s in comparison with the 1990s, J. Appl. Meteorol., 44, 1563–1573, 2005.
IEC62305 – The technical committee of the International Electrotechnical Commission: Protection against lightning, IEC, Geneva, Switzerland, 2006.
Kaplan, S. and Garrick, B. J.: On the quantitative definition of risk, Risk Anal., 1, 11–27, 1981.
Lopez, R. E. and Holle, R. L.: Changes in the number of lightning deaths in the United States during the twentieth century, J. Climate, 11, 70–77, 1997.
Lopez, R. E., Holle, R. L., Watson, A. I., and Skindlov, J.: Spatial and temporal distributions of lightning over Arizona from a power utility perspective, J. Appl. Meteorol., 36, 825–831, 1997.
Ma, M., Lu, W., Zhang, Y., Meng, Q., and Yang, J.: Characteristics of lightning exposure in China from 1997 to 2006, Chinese J. Appl. Meteorol. Sci., 19, 393–400, 2008.
Meyer, V., Sebastian, S., and Dagmar, H.: A multicriteria approach for flood risk mapping exemplified at the Mulde river, Germany, Nat. Hazards, 48, 17–39, 2009.
Mote, T. L., Lacke, M. C., and Shepherd, J. M.: Radar signatures of the urban effect on precipitation distribution: a case study for Atlanta, Georgia, Geophys. Res. Lett., 34, L20710. doi:10.1029/2007GL031903, 2007.
Orville Jr., R. E.: An analytical solution to obtain the optimum source location using multiple direction finders on a spherical surface, J. Geophys. Res., 92, 10877–10886, 1987.

NHESSD
1, 4115–4154, 2013

Petrov, N. I. and D'Alessandro, F.: Assessment of protection system positioning and models using observations of lightning strikes to structures, Proc. R. Soc. Lond. A, 458, 723–742. doi:10.1098/rspa.2001.0906, 2002.
Price, C. and Rind, D.: What determines the cloud-to-ground lightning fraction in thunderstorms?, Geophys. Res. Lett., 20, 463–466, doi:10.1029/93GL00226, 1993.
Renn, O.: Three decades of risk research: accomplishments and new challenges, J. Risk Res., 1, 49–71, 1998.
Rizk, F. A. M.: Modelling of lightning incidence to tall structures, part II, application, IEEE T. Power Deliver., 9, 172–193, 1994.
Rose, L. S., Stallins, J. A., and Bentley, M. L.: Concurrent cloud-to-ground lightning and precipitation enhancement in the Atlanta, Georgia (United States), urban region, Earth Interact., 12, 1–30, doi:10.1175/2008EI265.1, 2008.
Shepherd, J. M., Pierce, H., and Negri, A. J.: Rainfall modification by major urban areas: observations from spaceborne rain radar on the TRMM satellite, J. Appl. Meteorol., 41, 689–701, 2002.
Smith, K.: Environmental Hazards: Assessing Risk and Reducing Disaster, 2nd Edn., Routledge, New York, USA, 1996.
Sonia, A. A. and Gerard, B.: Lightning interception on elevated building, in: Proceedings of the 5th WSEAS Int. Conf. on Power Systems and Electromagnetic Compatibility, 23–25 August 2005, WSEAS, Corfu, Greece, 17–23, 2005.
Stallins, J. A. and Rose, L. S.: Urban lightning: current research, methods, and the geographical perspective, Geography Compass, 2, 620–639, doi:10.1111/j.1749-8198.2008.00110.x, 2008.
Tao, S. and Meng, Q.: Evaluation of ground stroke density distribution and lightning detection efficiency in Beijing-Tianjin-Hebei area, Acta Meteorol. Sin., 10, 346–335, 1996.
Tao, Z. and Zhao, X.: Climatological analysis of lightning in Beijing-TianJin-HeBei District, Acta Meteorol. Sin., 51, 325–332, 1993.
Vogt, B. J.: Exploring cloud-to-ground lightning earth highpoint attachment geography by peak current, Earth Interact., 15, 1–16, 2011.
Williams, E. R.: Lightning and climate: a review, Atmos. Res., 76, 272–287, 2005.
Wisdom, M. D.: Lightning fatalities in Swaziland: 2000–2007, Nat. Hazards, 50, 179–191, 2009.
Zhang, W., Meng, Q., Ma, M., and Zhang, Y.: Lightning casualties and damages in China from 1997 to 2009, Nat. Hazards, 57, 465–476, 2011.

Zheng, D., Meng, Q., Lu, W., Zhang, Y., Chai, X. and Ma, M.: Spatial and temporal characteristics of cloud-to-ground lightning in summer in Beijing and its circumambience regions, Chinese J. Appl. Meteorol. Sci., 16, 638–664, 2005.
Zhou, Y., Zhang, J., and Sun, L.: Statistic analysis on clound-to-ground lightning characteristics over Beijing, Tianjin and Hebei Province, J. Catastrophology, 24, 101–104, 2009.

NHESSD
1, 4115–4154, 2013

The characteristics of lightning risk and zoning in Beijing

H. Hu et al.

Table 1. The building types corresponding to the lightning protection characteristics in Beijing.

Building type	GIS identity code	Protection measure	protection measure to reduce physical damage	SPD level
general building	211	Iron infra-building and framework as a lead-in wire in the building	Protected by LPS III	No coordinated SPD protection
general building with basement	21 109	Same as above	Protected by LPS III	Same as above
bunk house	212	Effective soil equipotentialization	Not protected by LPS	Same as above
hunk house with basement	21 209	Same as above	Same as above	Same as above
bridge gallery	218	Electrical insulation of exposed down-conductor	Same as above	Same as above
Special house	229	Iron infra-building and framework as a lead-in wire in the building	Protected by LPS I	SPD II are designed
Special house with basement	22 909	Same as above	Same as above	SPD III are designed
Ruined house	214	No protection measures	Not protected by LPS	No coordinated SPD protection
Hut	215	Same as above	Same as above	Same as above
Public lavatory	3551	Electrical insulation of exposed down-conductor	Same as above	Same as above

NHESSD
1, 4115–4154, 2013

Table 2. The rule of estimating the open-field area location factor C_d corresponding with the terrain (quoted from IEC62305, 2006).

The bare space exposure and its sounding	C_d
Terrain that is 8 m higher within a range of 250 m	0.7
A 5 m elevation surge (standard deviation) within a range of 250 m	1
On the top or ridge of a mountain	1.5

NHESSD
1, 4115–4154, 2013

Table 3. Definition of the estimated ratio of the outdoor population in intervals within one day.

0–5 h	5–7 h	7–9 h	9–12 h	12–14 h	14–17 h	17–19 h	19–22 h	22–24 h
0 %	2 %	20 %	10 %	10 %	10 %	5 %	1 %	0.5 %

Discussion Paper | Discussion Paper | Discussion Paper | Discussion Paper |
NHESSD
1, 4115–4154, 2013
The characteristics of lightning risk and zoning in Beijing
H. Hu et al.

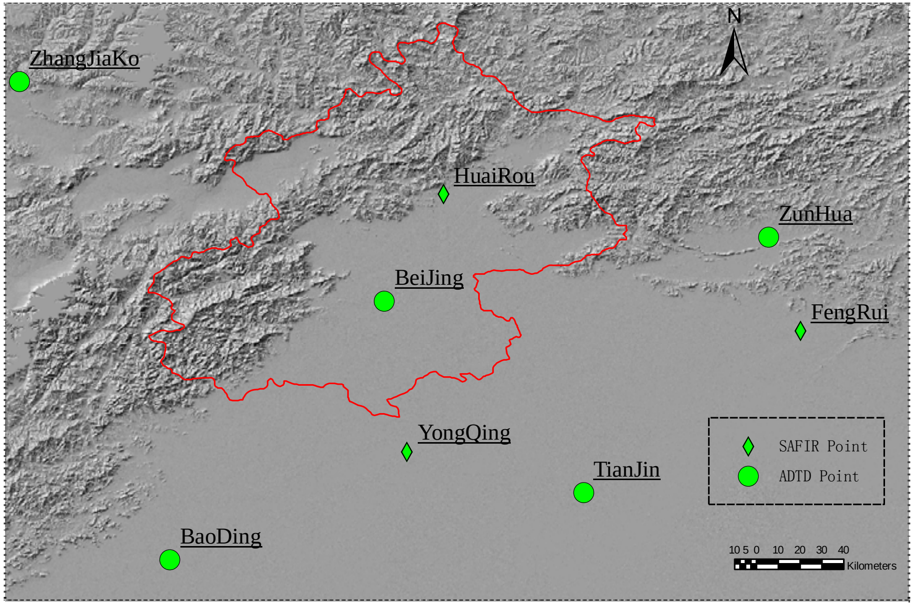

Fig. 1. The distribution map of SAFIR and ADTD detection stations around Beijing.

NHESSD
1, 4115–4154, 2013

The characteristics of lightning risk and zoning in Beijing

H. Hu et al.

Title Page
Abstract Introduction
Conclusions References
Tables Figures
◀ ▶
◀ ▶
Back Close
Full Screen / Esc
Printer-friendly Version
Interactive Discussion

NHESSD
1, 4115–4154, 2013

The characteristics of lightning risk and zoning in Beijing

H. Hu et al.

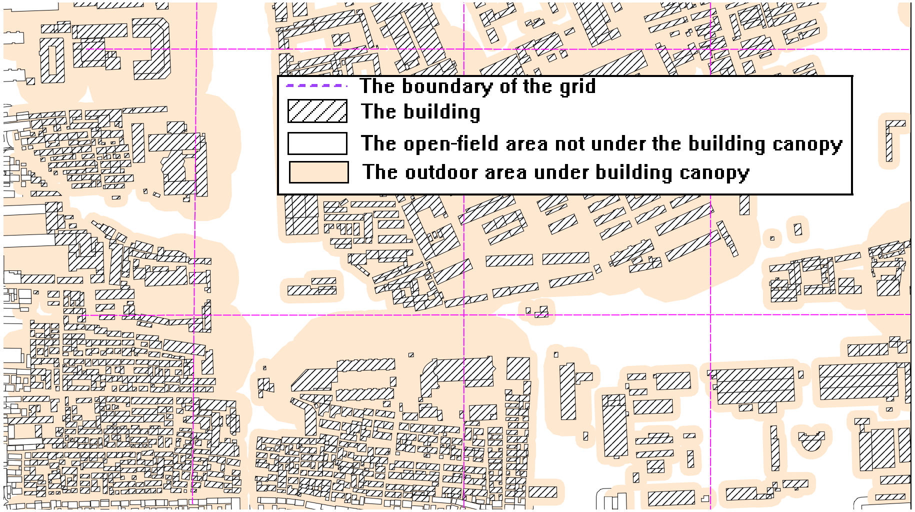

Fig. 2. The classification of the buildings, outdoor area under the building canopy and open-field area on the land surface and its samples in the grid cells.

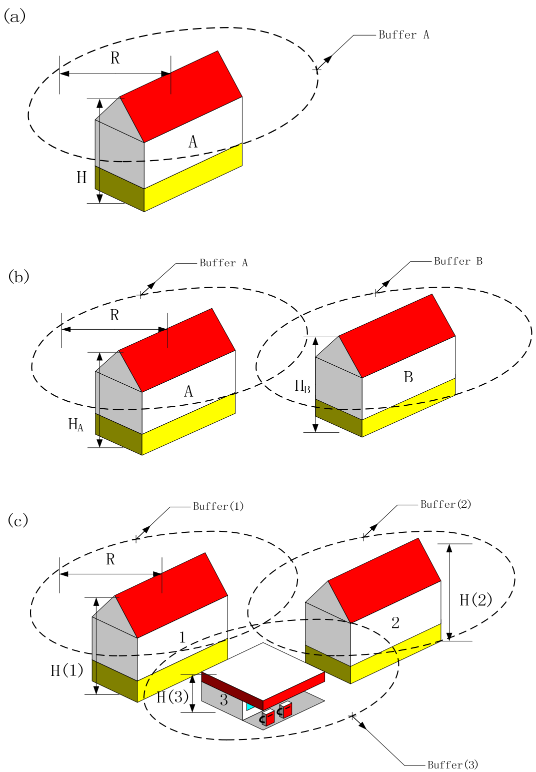

Fig. 3. The sketch of **(a)** a building with its covering distance of attraction radius, and its collection area, building A; **(b)** two neighboring buildings next to one another, and the collection areas of buildings A and B, which intersect with one another; **(c)** more than two neighboring buildings next to one another, and the collection areas of more than two buildings that intersect with one another.

NHESSD
1, 4115–4154, 2013

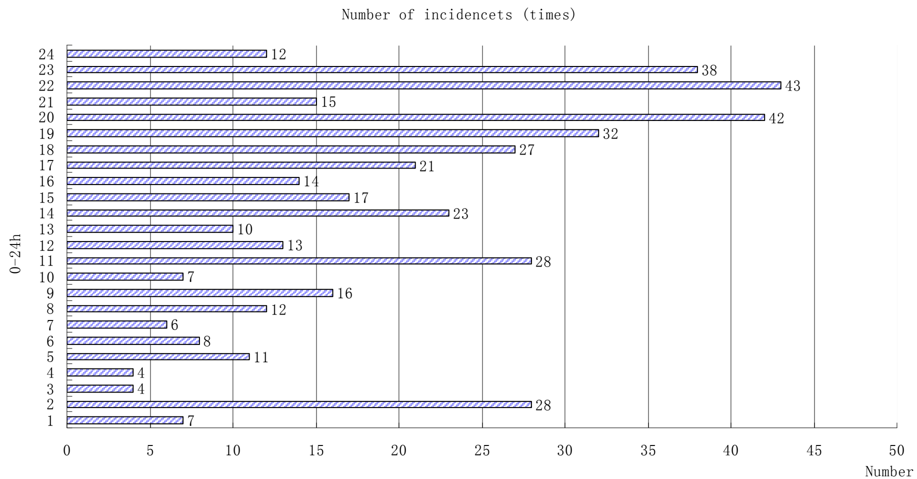

Fig. 4. The number of historical lightning incidents occurring at 0–24 h intervals in one day.

NHESSD
1, 4115–4154, 2013

The characteristics of lightning risk and zoning in Beijing

H. Hu et al.

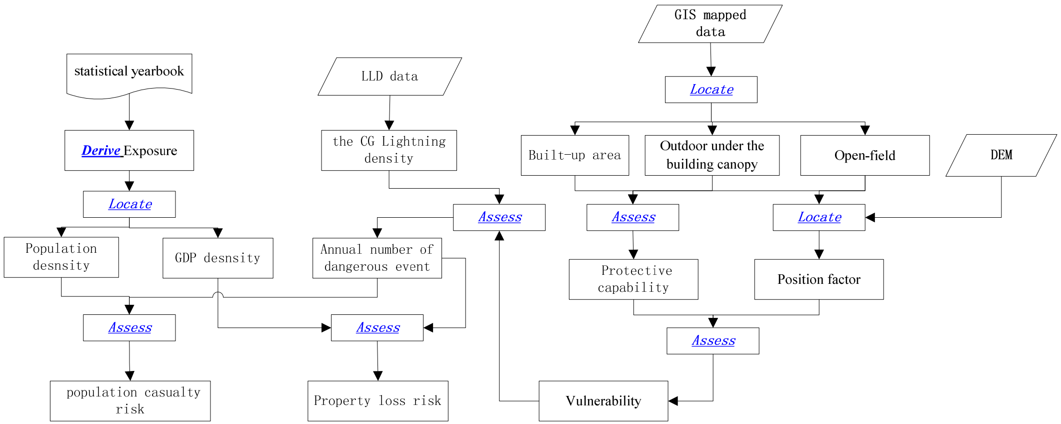

Fig. 5. Schematic display of framework for lightning risk assessment model.

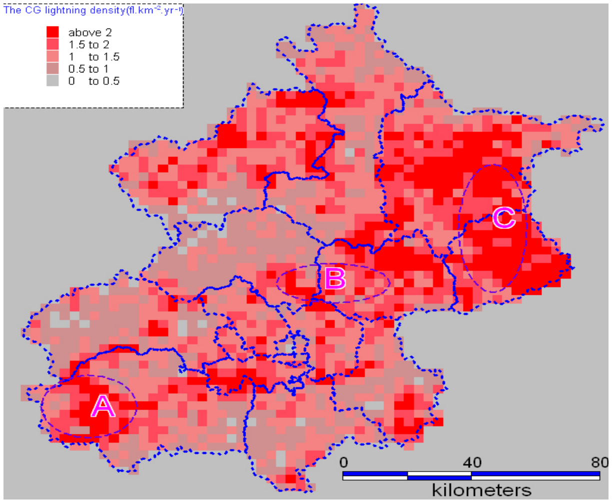

Fig. 6. The CG flash density distribution map derived from the lightning location finder data, indicating three high areas (A, B, C) in Beijing.

NHESSD
1, 4115–4154, 2013

The characteristics of lightning risk and zoning in Beijing

H. Hu et al.

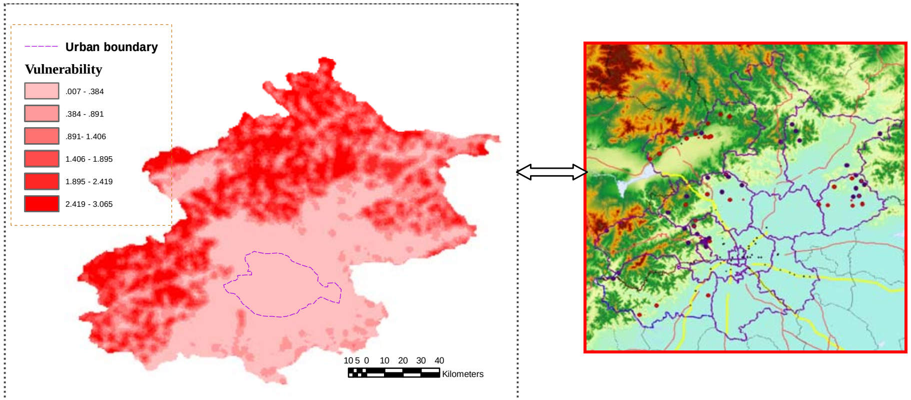

Fig. 7. The zoning of the vulnerability calculated by the model and its corresponding topography sketch in Beijing.

NHESSD
1, 4115–4154, 2013

The characteristics of lightning risk and zoning in Beijing

H. Hu et al.

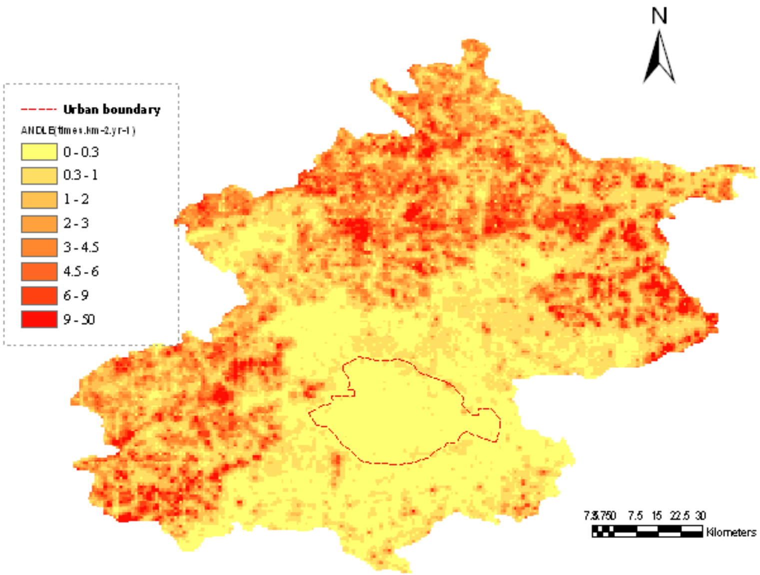

Fig. 8. The zoning of the Annual Number of Dangerous Lightning Event (ANDLE) simulated by the model.

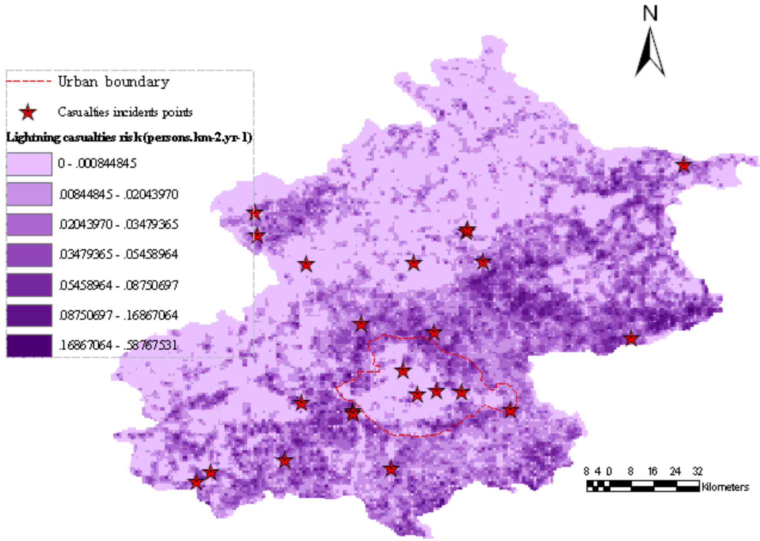

Fig. 9. The zoning of the lightning related casualty risk simulated by the model and the distribution of historical casualty incidents in Beijing.

NHESSD
1, 4115–4154, 2013

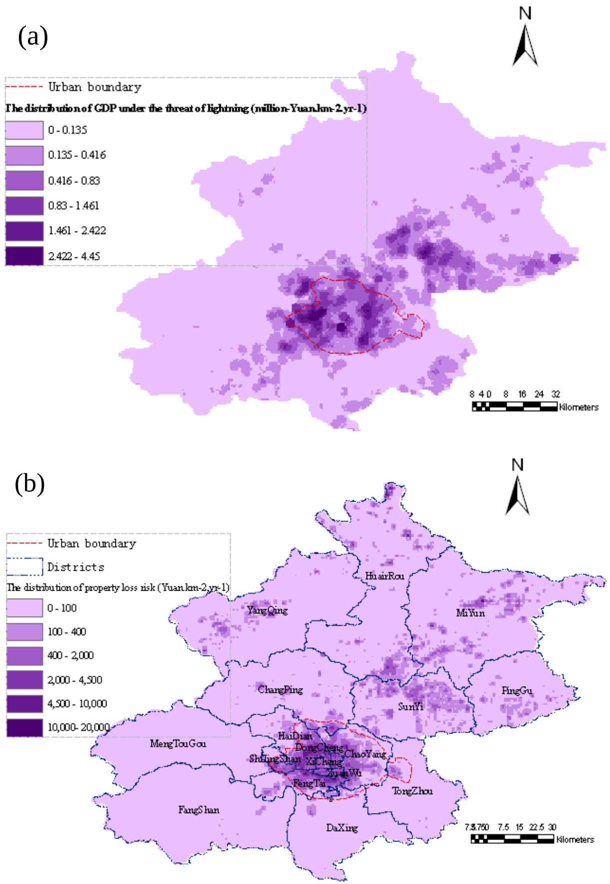

Fig. 10. The zoning of **(a)** the amount of GDP under the threat of lightning; **(b)** property loss risk simulated by the model.

NHESSD
1, 4115–4154, 2013

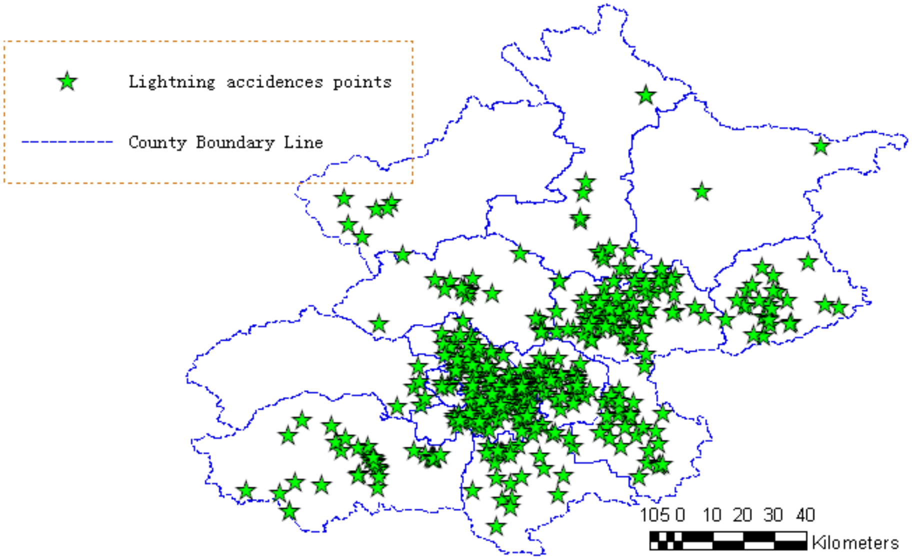

Fig. 11. The distribution of lightning incident points from 2001 to 2010 in Beijing.

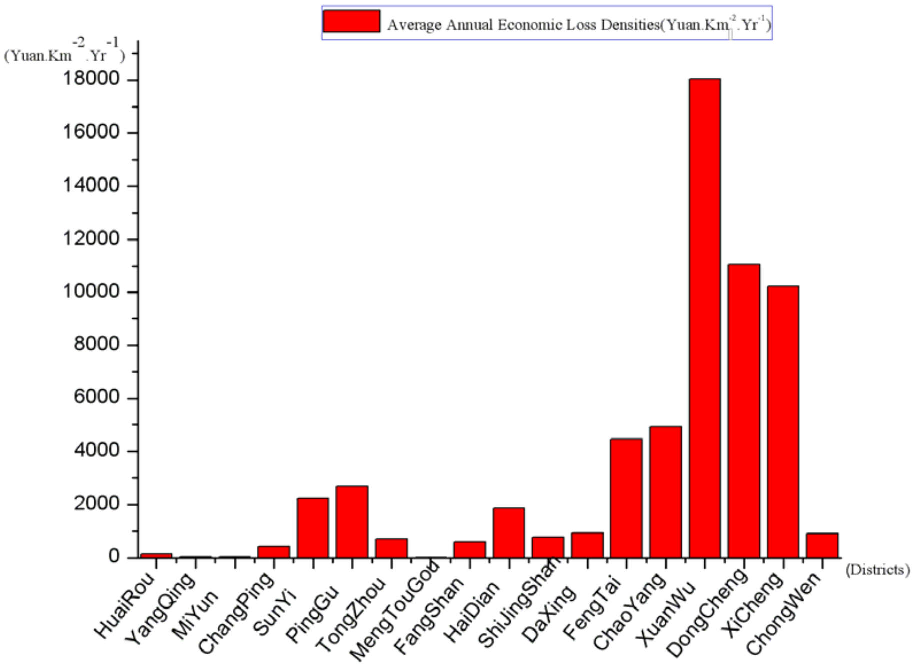

Fig. 12. The Average Annual Economic Loss Densities of the districts of Beijing.

NHESSD
1, 4115–4154, 2013